THE JOURNAL OF PHYSICAL CHEMISTRY C

Article

pubs.acs.org/JPCC

Nitrogen Plasma Surface Modification of Poly(3,4-ethylenedioxythiophene):Poly(styrenesulfonate) Films To Enhance the Piezoresistive Pressure-Sensing Properties

Jer-Chyi Wang,[*,†,‡,#,∇] Rajat Subhra Karmakar,[†] Yu-Jen Lu,[§,∇] Ming-Chung Wu,[∥] and Kuo-Chen Wei[⊥,∇]

[†]Department of Electronic Engineering, [‡]Biosensor Group, Biomedical Engineering Center, [§]School of Traditional Chinese Medicine, [∥]Department of Chemical and Materials Engineering, and [⊥]School of Medicine, Chang Gung University, Guishan District 33302, Taoyuan, Taiwan

[#]Department of Electronic Engineering, Ming Chi University of Technology, Taishan District 24301, New Taipei City, Taiwan

[∇]Department of Neurosurgery, Chang Gung Memorial Hospital, Guishan District 33305, Taoyuan, Taiwan

Supporting Information

ABSTRACT: A conductive polymeric film, poly(3,4-ethylenedioxythiophene):poly(styrenesulfonate) (PEDOT:PSS), is surface-modified by nitrogen plasma in order to enhance its piezoresistive characteristics. With an optimized 3 min nitrogen plasma surface modification, the piezoresistive sensitivity and response were significantly enhanced. Hall measurements and temperature-dependent conductance measurements are carried out to determine the electron-hopping behavior of nitrogen-plasma-modified PEDOT:PSS films, suppressing the horizontal carrier conducting pathway in the PEDOT:PSS piezoresistive pressure sensors. X-ray photoelectron spectroscopy (XPS) and Raman spectroscopy are applied to observe the PEDOT:PSS film surface after being modified with nitrogen plasma. The presence of sulfamate (SO_3−NH_2) and thiocyanate (S−C≡N) groups indicates a breaking of the electrostatic bonding between PEDOT and PSS and a modification of the conductive PEDOT conjugated chain. At the film surface, the formation of thiocyanate groups of PEDOT oligomers without the electrostatic bonding of PSS makes the PEDOT:PSS more hydrophobic, changing the surface characteristics of the PEDOT:PSS film. The newly formed less-conductive film surface alters the piezoresistance of PEDOT:PSS pressure sensors, implying their potential applications for future high-performance tactile sensing.

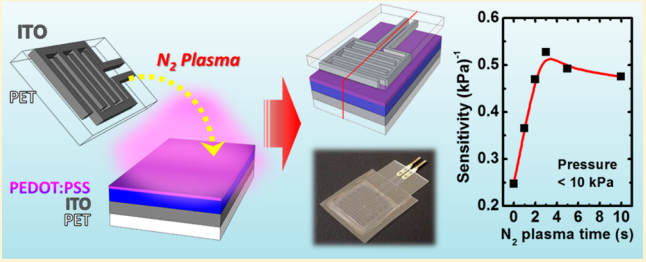

INTRODUCTION

Since the discovery of electrical conductivity in polyacetylene in the 1970s by the pioneering work of Shirakawa et al.,[1] conductive polymers have attracted a great deal of attention in both science and engineering communities. An organic polymer that possesses the electrical, magnetic, and optical properties of a metal, while also retaining the mechanical properties and easily processed nature associated with conventional polymers, it is known as an intrinsically conducting polymer and also known as a synthetic metal.[2] Conductive polymers have favorable behaviors with regards to metal−insulator transitions, flexibility, light weight, and low production cost,[3−5] allowing for their use in biosensors,[6] light-emitting diodes,[7] photovoltaic cells,[8] and field-effect transistors.[9] The conductivity of conductive polymers, which are characterized by a backbone chain of alternating double and single bonds, spans a very wide range of 10^{-12}−10^{4} S·cm^{-1}.[10,11] The integrated advantages of conjugated polymers with functional properties such as absorption and emission of light (which can change the conductivity) make it possible to use these materials in innovative optoelectronics. Furthermore, the overlapping p-orbitals create a system of delocalized π-electrons, which can result in interesting and useful electronic properties.[12]

Among the conductive polymers currently known, poly(3,4-ethylenedioxythiophene):poly(styrenesulfonate) (PEDOT:PSS) has emerged as one of the most technologically important materials in current plastic electronics due to its high electrochemical and thermal stability, high conductivity, favorable optical properties, and high transparency.[13,14] PEDOT is a conductive polymer based on 3,4-ethylenedioxythiophene (EDOT) monomer. To balance the cationic charge of PEDOT and allow for the dispersion of PEDOT in water, polystyrene sulfonic acid (PSS) is introduced to form the water-soluble PEDOT:PSS polymer.[14] Thus, PEDOT:PSS has been used in antistatic coatings,[15] as electrically conducting coatings,[16] as a transparent conductor in electroluminescent devices,[17] as a conducting layer in capacitors,[18] in printed wiring board manufacturing,[15] and as the hole injection layer in organic light-emitting diode (OLED),[19] in photovoltaics,[20] and

Received: September 23, 2016
Revised: October 31, 2016
Published: November 2, 2016

DOI: 10.1021/acs.jpcc.6b09642
J. Phys. Chem. C 2016, 120, 25977−25984

in organic thin-film transistors.[21] Previous studies have also shown that PEDOT can be applied in the development of microelectrodes for neural interfaces[22] as well as in scaffolds for epithelial cell adhesion and proliferation controlled by electrochemical modulation of surface properties;[23] the extent of these applications indicates the biocompatibility of PEDOT films. Generally speaking, pristine PEDOT:PSS has a very low conductivity of less than 1 $S{\cdot}cm^{-1}$,[24] which is caused by the PSS. The PSS, which can act on its own as the counterion, is an insulator.[25] Consequently, in order to make this material useable as an electrode, a great deal of research has been devoted to enhancing the conductive properties of PEDOT:PSS by using post-fabrication treatments, material processing, and impurity doping to optimize the structural and molecular order.[26] As a result, chemically altered PEDOT:PSS offers higher conductivity and has been used in a number of applications due to these improved characteristics.[27,28]

Recently, PEDOT:PSS has presented unique piezoresistive characteristics and has been applied in pressure and tactile sensing by using polyimide and flexible poly(ethylene terephthalate) (PET) substrates.[29] Interdigitated electrode (IDE) structure with feature sizes on the nanometer scale is currently quite popular in the electronics industry. It has been implemented in various devices, including surface acoustic wave sensors,[30] chemical sensors,[31] microelectromechanical systems biosensors,[32] and semiconducting nanowires.[33] Previously, different electrode structures of IDEs and cross-point electrodes (CPEs) were implemented in PEDOT:PSS pressure sensors to investigate the basic piezoresistive characteristics.[34] The structure-dependent piezoresistive properties provide preliminary experimental data on the PEDOT:PSS pressure sensors, proving the use of these structures in pressure- and tactile-sensing applications. To be used in the piezoresistive field, PEDOT:PSS films with sufficiently low conductivity in the absence of applied force and rapid increase of conductivity during the application of force are needed to obtain the superior and necessary piezoresistive properties. In this work, the material, physical, and piezoresistive characteristics of PEDOT:PSS films are investigated after nitrogen plasma surface modification. The piezoresistive performances of the PEDOT:PSS pressure sensors have been enhanced and optimized by a 3 min nitrogen plasma surface modification. Chemical changes at the PEDOT:PSS film surface, determined using X-ray photoelectron spectroscopy (XPS) and Raman spectroscopy, lead to changes in the piezoresistive behavior of PEDOT:PSS pressure sensors. The carrier conductive mechanism of such films is confirmed by Hall measurements and temperature-dependent conductance measurements, which demonstrate the improved piezoresistive sensing properties of PEDOT:PSS pressure sensors using the surface plasma treatment technology.

EXPERIMENTAL SECTION

Sample Preparation. Piezoresistive pressure-sensing devices with IDE structure were fabricated on flexible PET substrates with an indium−tin oxide (ITO) layer. The thickness of PET and ITO films was 200 and 0.35 μm, respectively. ITO was used as the electrode material, due to its advantages of high electron density (10^{21} cm^{-3}) in the conduction band and sufficient stability in aqueous solution for electrochemical applications.[35] Further, ITO is transparent to visible light, which enables multiple parameter measurements using optical and electrical techniques.[36] The pressure-sensing device (Figure 1b) is a combination of two parts, a plasma-modified

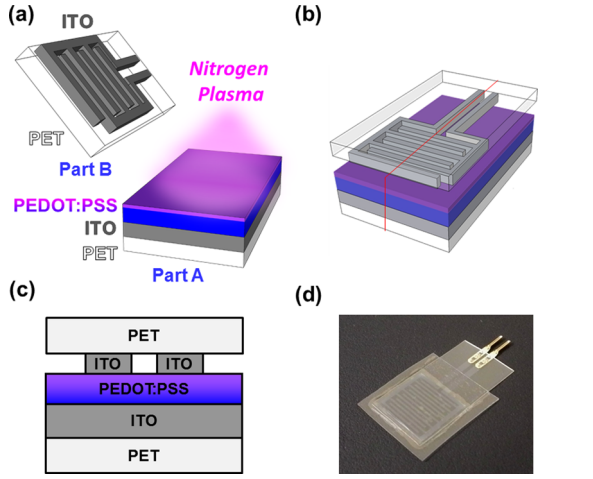

Figure 1. Schematic diagrams of the PEDOT:PSS pressure sensor after nitrogen plasma surface modification for (a) parts A and B, (b) the final device, and (c) the cross-sectional view of pressure sensor. An image of a fabricated device is shown in panel d. Nitrogen plasma modification was performed on the PEDOT:PSS film surface of part A.

PEDOT:PSS film (part A) and a patterned interdigitated ITO electrode (part B), as presented in Figure 1a. The width and spacing of each finger is 500 μm, and the active cell area of the sensors is 0.6825 cm^2. The interdigitated pattern was transferred to ITO electrode via conventional photolithography. Due to the hydrophobic nature of ITO, O_2 plasma treatment was performed for 2 min to make a hydrophilic film surface.[37] Then, the PEDOT:PSS was spin-coated on PET−ITO substrates at a spin speed of 500 rpm to obtain an average film thickness of 1.88 μm using an α-step profilometer (Dektak XT surface profiler, Bruker Corp.) with at least 20 fabricated films. In this study, a 1.6 wt % PEDOT:PSS solution was purchased from Heraeus, by the trade name of CLEVIOS P VP AI 4083, to have a resistivity of 7.85×10^2 $\Omega{\cdot}cm$,[38] which is on the same order of magnitude for the samples with a PEDOT:PSS ratio of 1:6.[39] All films were baked at 120 °C on a hot plate to evaporate excess solvent and increase film resilience. After that, nitrogen plasma surface modification was carried out on the PEDOT:PSS film surface in a plasma-enhanced chemical vapor deposition (PECVD) system at a power of 50 W for 1−10 min. Finally, parts A and B in Figure 1a were combined and packaged using a commercial PET material. The package technique is used to reduce the issues raised by the not entirely intimate contact between the top ITO electrode and PEDOT:PSS layer. The cross-sectional structure of the PEDOT:PSS pressure sensor is illustrated in Figure 1c, obtained from the cut-line of Figure 1b. The image of the fabricated PEDOT:PSS pressure sensor is shown in Figure 1d.

Characterization. Surface modifications of PEDOT:PSS films were examined using XPS analysis (ULVAC-PHI 5000 Versaprobe II system, ULVAC-PHI Inc.), Raman spectroscopy (Micro Raman/PL/TR-PL spectrometer, ProTrustech Co., Ltd.), and Hall measurements (BioRad HL5500 Hall measurement system, Nanometrics Inc.). The electrical properties were characterized using a Keithley 2450 interactive digital source meter (Keithley Instruments Inc.). In addition, the variable range hopping (VRH) measurement was performed using a

DOI: 10.1021/acs.jpcc.6b09642
J. Phys. Chem. C 2016, 120, 25977−25984

cryogenic prober station (CG-196CU, EverBing Int'l Corp.). The samples were placed on a homemade sample holder, and the pressure was applied using a JSV H1000 vertical stand (Japan Instrumentation System Co., Ltd.) equipped with a force gauge. A quartz buffer layer of 1 cm^2, larger than that of the active area, was used to apply equal pressure throughout the whole sensor device. A pressure of 0.1−20 kPa was applied on the samples to obtain the piezoresistive characteristics. The flowchart for the piezoresistive measurement algorithm of PEDOT:PSS pressure sensors is illustrated in Figure S1 of the Supporting Information.

RESULTS AND DISCUSSION

Piezoresistive Behavior. Figure 2a graphically demonstrates the resistance versus pressure (R−P) behavior of

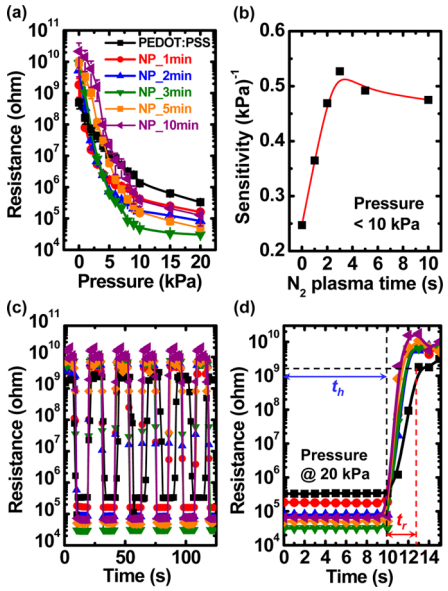

Figure 2. (a) R−P characteristics of the PEDOT:PSS pressure sensors after nitrogen plasma surface modification. (b) Piezoresistive sensitivity of pressure sensors at an applied pressure lower than 10 kPa. (c) Reversible testing of pressure sensors for at least five loops. A pressure of 20 kPa applied under a 10-s holding time (t_h) was used for these measurements. (d) R−t behavior after pressure release. The relaxation time (t_r) is defined as the waiting time required to reach a resistance of 1 GΩ after the normal pressure is released.

PEDOT:PSS pressure sensors after nitrogen plasma surface modification. To obtain the statistical distribution, at least 20 samples were measured for each pressure sensor. The piezoresistive sensitivity of these samples can be acquired by calculating the slope of the curves at a pressure lower than 10 kPa, which is the starting pressure of response saturation in Figure 2a, as presented in eq 1 and summarized in Table S1 (Supporting Information)

$$S = \frac{\log(R_0) - \log(R_{10\,\mathrm{kPa}})}{10\ \mathrm{kPa}} \quad (1)$$

where S is the piezoresistive sensitivity, R_0 is the resistance without any pressure applied, and $R_{10\,\mathrm{kPa}}$ is the resistance at 10 kPa. With the increase of nitrogen plasma treatment time, the piezoresistive sensitivity first increases and then decreases, as shown in Figure 2b. The sensitivity can be optimized to be 0.527 kPa^{-1} for the PEDOT:PSS pressure sensors with nitrogen plasma surface modification for 3 min. Figure 2c shows the reversible testing of the PEDOT:PSS pressure sensors after nitrogen plasma surface modification for at least five loops. A pressure of 20 kPa applied under a 10-s holding time (t_h) was used for these measurement. All samples present a stable resistive switching for 2 min sequential and reversible operations. To further investigate the piezoresistive response of these materials, the resistance versus time (R−t) behavior of the pressure sensors after pressure release is displayed in Figure 2d. The relaxation time (t_r) is defined as the waiting time required to reach a resistance of 1 GΩ after the normal pressure is released, which can be calculated using eq 2 and is summarized in Table S1 of the Supporting Information

$$t_r = t_{1\,\mathrm{G\Omega}} - t_h \quad (2)$$

where $t_{1\,\mathrm{G\Omega}}$ is the time required for the resistance to reach 1 GΩ and t_h is the holding time (10 s). This figure demonstrates that the relaxation time of PEDOT:PSS pressure sensors is significantly reduced after the nitrogen plasma surface modification.

Physical Properties. Figure 3 shows the VRH distance and carrier mobility of PEDOT:PSS films with different nitrogen

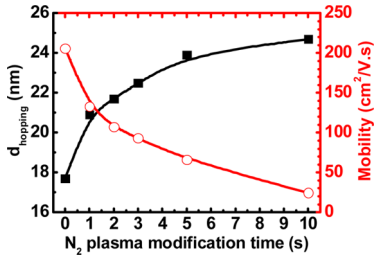

Figure 3. Variable range hopping (VRH) distance and carrier mobility of PEDOT:PSS films with different nitrogen plasma treatment times.

plasma modification times. The hopping distance is determined from the temperature-dependent conductance, $G(T)$, of PEDOT:PSS films (Supporting Information, Figure S2a), which can be described by Mott's law[40]

$$G(T) = G_0 \exp[-(T_0/T)^{\gamma}] \quad (3)$$

where G_0 is the conductance prefactor, T_0 is the characteristic temperature, T is the measurement temperature (230−300 K), and γ is an exponent related to the transport process. In the usual analysis of VRH transportation, the exponent γ equals $1/(d + 1)$, where d is the dimensionality of the electrical conduction path.[41] Hence, $\gamma = {}^1/_4$ indicates a three-dimensional variable-range hopping, and the conductance versus $T^{1/4}$ characteristics are linearly fitted to extract T_0 (Supporting Information, Figure S2b). The linear fitting seems to be a departure when the PEDOT:PSS films are modified by the nitrogen plasma. The departure may be due to the plasma-damage-induced leakage current. In Figure S2b, there appears to be a conductance limitation of approximately 9×10^{-8}−10^{-7} S, which resulted from the leakage current. When the nitrogen plasma treatment time increases, the conductance of the PEDOT:PSS film decreases; thus, the departure from a linear response will become greater. To obtain the intrinsic hopping characteristics, the conductance values higher than the portion by leakage current are used for the linear fitting. Then, the extracted T_0 is related to the density of states at the Fermi level, $g(E_F)$, via eq 4

DOI: 10.1021/acs.jpcc.6b09642
J. Phys. Chem. C 2016, 120, 25977−25984

$$T_0 = \frac{\beta}{g(E_F)\xi^3 k_B} \quad (4)$$

where ξ is the localization length, β is a numerical factor with the value of 21.2, and k_B is the Boltzmann constant.[40] $g(E_F)$ can be extracted on the basis of T_0, and the hopping distance (l_0) can be obtained from eq 5[42]

$$l_0 = \left\{ \frac{3}{2\alpha\left(\frac{4\pi}{3}\right) g(E_F) k_B T} \right\}^{1/4} \quad (5)$$

where α is the rate of decay of the wave function, which is related to ξ using eq 6

$$\alpha = 1/\xi \quad (6)$$

In the figure, the PEDOT:PSS films with and without nitrogen plasma surface modification present the hopping distance of 17.7−24.6 nm, which is of the same magnitude as that observed by Nardes et al.[43] The increment in hopping distance is determined as a function of the nitrogen plasma surface modification time. Furthermore, the carrier mobility is significantly decreased after nitrogen incorporation. The changes in the variable range hopping distance and carrier mobility can be ascribed to the chemical changes of the PEDOT:PSS film surface after nitrogen plasma treatment.

Figure 4 displays the wetting ability of water for the PEDOT:PSS films with and without nitrogen plasma surface

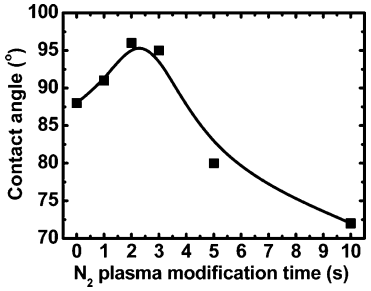

Figure 4. Contact angle versus the time of nitrogen plasma surface modification of PEDOT:PSS films.

modification. The water contact angle images shown in Figure S3a−f (Supporting Information) were measured using the sessile drop method with a water droplet partially wetting the PEDOT:PSS films.[44] It can be found that the water contact angle of the original PEDOT:PSS film was 88°. After nitrogen plasma surface modification for 3 min, the PEDOT:PSS film possesses a much higher water contact angle (95°) than the unmodified film. Previous studies have indicated that the changes in the hydrophobicity of PEDOT:PSS films with poly(butyl acrylate) (PBA) are linked to changes in the film composition and structure,[45] which are observed at the surface of our nitrogen-plasma-modified PEDOT:PSS films and will be discussed later. Further, for the PEDOT:PSS films with a nitrogen plasma surface modification of more than 3 min, the water contact angle decreases dramatically and the film becomes more hydrophilic due to the plasma damage at the PEDOT:PSS film surface.

Chemical Analysis. XPS and Raman spectra were measured to determine the surface chemical composition of PEDOT:PSS films modified by nitrogen plasma for 3 min. High-resolution peak areas, line shapes, and intensities of the S 2p, C 1s, and O 1s core level spectra are presented in Figure 5a. The position of the binding energy scale was adjusted to set the

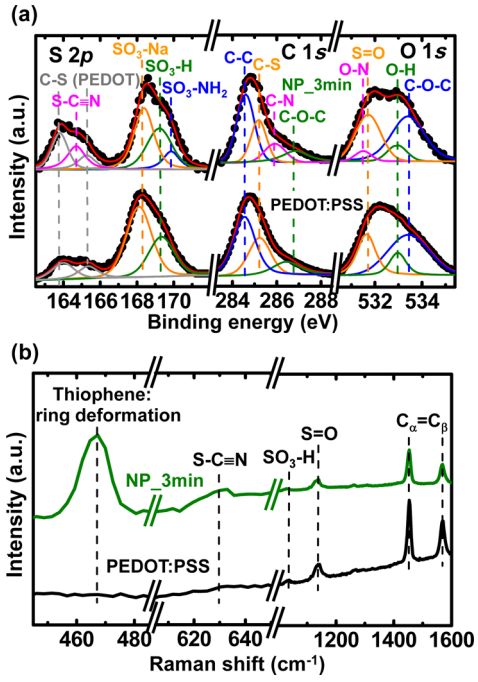

Figure 5. (a) XPS and (b) Raman spectra of PEDOT:PSS films after nitrogen plasma surface modification. The formation of sulfonamide (SO_2-NH_2) and thiocyanate (S−C≡N) for nitrogen-plasma-modified PEDOT:PSS films can be observed by XPS and Raman analyses.

main C 1s feature (C−C) at 284.6 eV.[46] For the S 2p spectra of the pure PEDOT:PSS film, there are two binding energy components observed around 164.0 and 168.2 eV, which indicate PEDOT and PSS respectively.[47,48] The S 2p contributing peaks at 163.9 and 165.3 eV result from the spin-split doublets of the sulfur atoms in PEDOT. On the other hand, the S signals from PSS are present at 166.5−171.0 eV because high-electronegative oxygen atoms attach to sulfur fragments of PSS.[49] The higher binding energy component of the S 2p peak at 169.2 eV (green line, Figure 5a) is associated with the SO_3-H group of PSS, whereas the lower binding energy component of the S 2p peak at 168.1 eV (orange line, Figure 5a) corresponds to the SO_3^- group of PSS.[50] For the samples with nitrogen plasma surface modification for 3 min, an extra peak is present at 169.9 eV, possibly corresponding to the SO_3-NH_2 of PSS. In addition, another peak at 164.7 eV could be ascribed to the S−C≡N group generated in PEDOT oligomer after nitrogen plasma surface modification.[51]

For the C 1s spectra of PEDOT:PSS films, three components are present at binding energies of 284.6, 285.2, and 286.8 eV, denoting C−C, C−S and C−O−C bonds, respectively.[48] An additional peak is present in the nitrogen-plasma-modified PEDOT:PSS film at 285.9 eV, which indicates modification of the C−N groups in the EDOT monomer.[52] Besides, the O 1s peaks of the spectra reveal three major components for the PEDOT:PSS film at 531.7, 533.0, and 533.4 eV, corresponding to S═O, O−H, and C−O−C bonds, respectively.[53,54] The intensity of the C−O−C peak is the highest among these, indicating the existence of the EDOT monomer. For the samples with nitrogen plasma surface modification for 3 min,

DOI: 10.1021/acs.jpcc.6b09642
J. Phys. Chem. C 2016, 120, 25977−25984

Scheme 1. Molecular Structure of PEDOT:PSS (a) without and (b) with Nitrogen Plasma Surface Modification

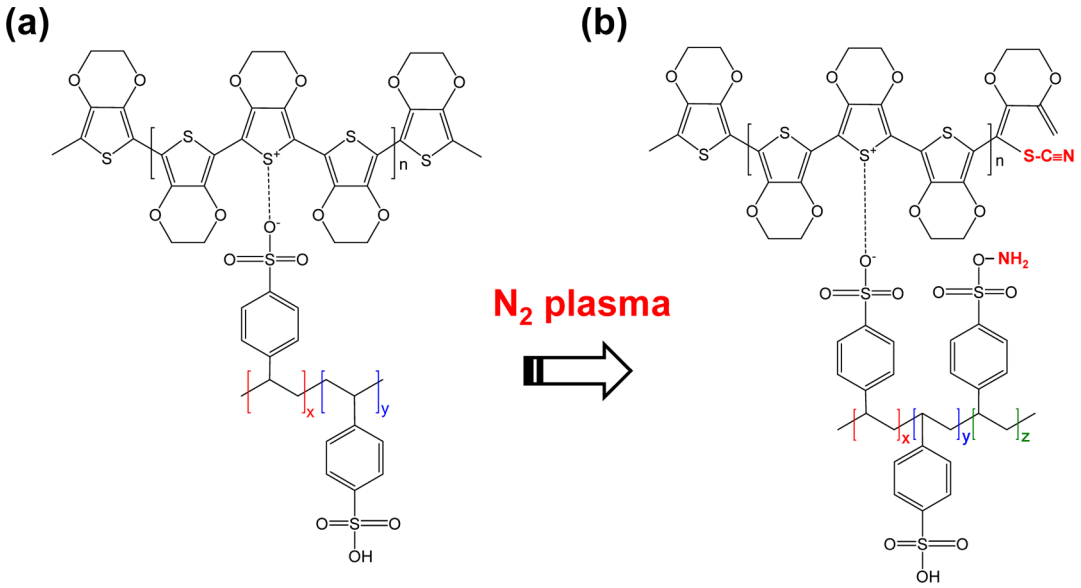

the presence of an extra component at 531.4 eV is linked to the formation of the O−N bond in PSS.[55] From the XPS analyses, it is evident that the chemical change takes place in both PEDOT and PSS after nitrogen plasma surface modification, leading to the breaking of the electrostatic bonding between PEDOT and PSS and the modification of the conductive PEDOT conjugated chains. Thus, the PEDOT:PSS film surface becomes rough as a result of the treatment, as shown in the atomic force microscopy (AFM) images of Figure S4 in the Supporting Information.

To further investigate the mechanism of chemical change in PEDOT:PSS films after nitrogen plasma surface modification, Raman spectra were collected and displayed in Figure 5b. These data show that the most obvious spectral changes occur at 1452 and 1524 cm^{-1}, representing the $C_\alpha{=}C_\beta$ symmetrical and asymmetrical stretching vibrations of the pure PEDOT:PSS films, respectively.[48,55−57] In addition, the vibrational modes at 1040 and 1140 cm^{-1} belong to the SO_3−H (PSS) and S=O, respectively.[56] After nitrogen plasma surface modification for 3 min, a new peak emerges at 630 cm^{-1}, denoting the S−C stretch. There is another new stretch at 467 cm^{-1} belonging to the ring deformation of thiophene.[46] These new modes indicate possible chemical changes in the thiophene rings of PEDOT oligomers, i.e., the formation of the thiocyanate groups (S−C≡N). The thiocyanate groups are only observed in nitrogen-plasma-modified samples, clearly demonstrating the nitrogen incorporation in the PEDOT:PSS film surface.

Chemical Modifications. In general, PEDOT:PSS films consist of PEDOT:PSS micelles with a core−shell structure (PEDOT as the core and PSS as the shell).[58] Nitrogen plasma treatment of PEDOT:PSS micelles modifies both the PEDOT oligomers and PSS chains. The material properties of nitrogen-plasma-modified PEDOT:PSS micelles are changed significantly, as displayed in Figure 5. The chemical structures of PEDOT:PSS micelles before and after nitrogen plasma modification are shown in parts a and b of Scheme 1, respectively. It is suggested that the electrostatic bonding is broken because of the nitrogen plasma surface modification. Traditionally, charged particles of molecular N_2^+ ions are abundant in nitrogen plasma environments[59] and will effectively react with the PEDOT:PSS chains. Because of this, the thiophene rings of PEDOT can be chemically modified to form the thiocyanate groups (S−C≡N). PEDOT itself is a conductive polymer, and the source of its conductive nature comes from its conjugated backbone. After nitrogen plasma surface modification, the conjugated chain of PEDOT is modified by the thiocyanate groups; consequently, the carrier transportation is interrupted due to the reduction of carrier mobility and the increase of 3D VRH distance, as shown in Figure 3. Also, the formation of sulfamate (SO_2−NH_2) in the nitrogen-plasma-modified PEDOT:PSS micelles indicates the electrostatic bond breakage. Besides, due to the formation of thiocyanate groups of PEDOT oligomers without the electrostatic bonding of PSS, the nitrogen-plasma-modified PEDOT:PSS becomes more hydrophobic,[60,61] as revealed in the contact angles of Figure 4.

Physical Mechanisms. For the carrier transportation of PEDOT:PSS film, it is reported that in the horizontal direction, the PEDOT-rich lamellas are only separated by the not completely closed constrictions, allowing carriers to hop to non-nearest-neighbor sites through a thin or nonexistent barrier and achieving a resistivity of 6.22×10^7 Ω·cm.[34,41] On the other hand, in the vertical direction, the PEDOT-rich domains are separated by thick PSS-lamella barriers, enforcing only nearest-neighbor hopping with a resistivity of 1.79×10^{11} Ω·cm. Thus, for the device with a thin PEDOT:PSS film of 1.88 μm and a wide finger spacing of 500 μm, both horizontal and vertical pathways of carrier conduction, i.e. paths 1 and 2 in Figure 6a, respectively, can be observed for the PEDOT:PSS pressure sensors with IDE structure, resulting in the slow response.[34] Further, the resistance modification of PEDOT:PSS films with and without force applied is responsible for the sensitivity enhancement of PEDOT:PSS pressure sensors modified by nitrogen plasma, as shown in Figure 2b. First of all, the initial resistance value (resistance without any pressure) increases as the nitrogen plasma treatment time increases (Figure 2a). This enhancement can be attributed to the modification of PEDOT conjugated chains at the PEDOT:PSS film surface by nitrogen plasma treatment, decreasing the surface carrier mobility and increasing the hopping distance, as shown in Figure 3. Thus,

DOI: 10.1021/acs.jpcc.6b09642
J. Phys. Chem. C 2016, 120, 25977−25984

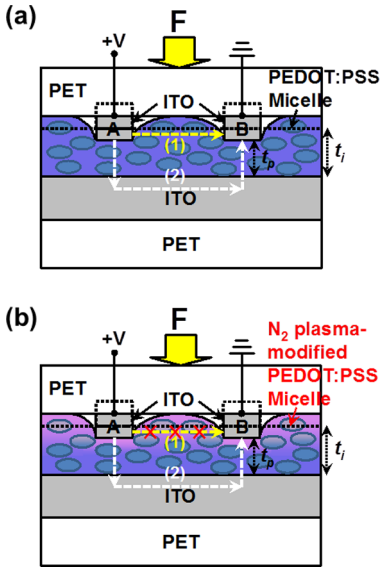

Figure 6. Schematic diagrams of carrier conducting pathways of PEDOT:PSS pressure sensors (a) without and (b) with nitrogen plasma surface modification.

the horizontal carrier conducting pathway is effectively suppressed (Figure 6b), presenting the high initial resistance value.[41] When a normal pressure is applied, the measured resistance of PEDOT:PSS pressure sensors decreases due to the more closely arranged PEDOT micelles of compressed film, demonstrating the well-known piezoresistive characteristics. When a high normal pressure (>10 kPa) is applied to the pressure sensors, it will contribute to the lowest value of measured resistance, which is strictly influenced by the nitrogen plasma treatment. Compared to the original film, the PEDOT:PSS pressure sensor after a nitrogen plasma surface modification of less than 3 min shows a decrease of its lowest resistance due to the broken electrostatic bonding between the positively charged PEDOT and negatively charged PSS, reducing the Coulomb interaction between them and helping to increase the conductivity of PEDOT:PSS film during the force applied.[62] Hence, the piezoresistive sensitivity is effectively enhanced for the nitrogen-plasma-modified samples. In addition, a single carrier conducting pathway in the vertical direction can hasten the return of the resistance to its initial value when the normal pressure is released, leading to the short relaxation time of the $R-t$ curve. With a nitrogen plasma treatment of more than 3 min, the modification of PEDOT conjugated chains becomes much more significant. Too much nitrogen incorporation will modify the PEDOT conjugated chains not only at the film surface but in the bulk of the PEDOT:PSS films, increasing the lowest resistance and reducing the piezoresistive sensitivity. Therefore, the piezoresistive performances of the PEDOT:PSS pressure sensors with nitrogen plasma modification are optimized at 3 min, which is suitable for future high-performance pressure-sensing applications.

CONCLUSIONS

Nitrogen plasma surface modification of PEDOT:PSS films has been investigated in the hopes of enhancing the piezoresistive characteristics of these films. XPS and Raman spectra were collected to determine the formation of sulfamate (SO_2-NH_2) and thiocyanate groups (S−C≡N), altering the electrostatic bonding between PEDOT and PSS, the PEDOT conjugated chains, and the surface morphology of nitrogen-plasma-modified PEDOT:PSS films. To understand the carrier conductive mechanism, Hall measurements and temperature-dependent conductance measurements were examined to realize the modification of variable-range hopping at the PEDOT:PSS film surface. Thus, the piezoresistive sensing behaviors of PEDOT:PSS pressure sensors, such as sensitivity and response, were significantly improved by nitrogen plasma surface modification, making high-performance pressure sensing possible.

ASSOCIATED CONTENT

Supporting Information

The Supporting Information is available free of charge on the ACS Publications website at DOI: 10.1021/acs.jpcc.6b09642.

Flowchart for piezoresistive measurement algorithm, curve fitting to obtain the hopping distance, contact angle images by the sessile drop method with a water droplet partially wetting the PEDOT:PSS films, AFM images of the surface morphology, and table summarizing piezoresistive characteristics (Figures S1−S4 and Table S1) (PDF)

AUTHOR INFORMATION

Corresponding Author

*Tel.: +886-3-2118800, ext 5784. Fax: +886-3-2118507. E-mail: jcwang@mail.cgu.edu.tw.

Notes

The authors declare no competing financial interest.

ACKNOWLEDGMENTS

This research was supported by Ministry of Science and Technology, R.O.C (Contract Nos. of MOST 103-2221-E-182-061-MY3 and MOST 105-2628-E-182-001-MY3), and Chang Gung Memorial Hospital, Taiwan (Contract Nos. of CMRPD2E0031, CMRPD2F0121, and BMRPA74). The authors would like to thank the Department of Neurosurgery, Chang Gung Memorial Hospital, Taiwan, and Dr. Pi-Chun Juan, Ming Chi University of Technology, Taiwan, for their technical support.

REFERENCES

(1) Shirakawa, H.; Louis, E. J.; MacDiarmid, A. G.; Chiang, C. K.; Heeger, A. J. Synthesis of Electrically Conducting Organic Polymers: Halogen Derivatives of Polyacetylene, $(CH)_x$. *J. Chem. Soc., Chem. Commun.* **1977**, *16*, 578−580.

(2) MacDiarmid, A. G. Synthetic Metals": A Novel Role for Organic Polymers (Nobel Lecture). *Angew. Chem., Int. Ed.* **2001**, *40*, 2581−2590.

(3) Skotheim, T.; Reynolds, J. *Handbook of Conducting Polymers*, 3rd ed.; CRC Press: Boca Raton, FL, 2007.

(4) Gardner, J. W.; Bartlett, P. N. Application of Conducting Polymer Technology in Microsystems. *Sens. Actuators, A* **1995**, *51*, 57−66.

(5) Dong, B.; Lu, N.; Zelsmann, M.; Kehagias, N.; Fuchs, H.; Sotomayor Torres, C. M.; Chi, L. Fabrication of High-Density, Large-Area Conducting-Polymer Nanostructures. *Adv. Funct. Mater.* **2006**, *16*, 1937−1942.

(6) Gerard, M.; Chaubey, A.; Malhotra, B. D. Application of Conducting Polymers to Biosensors. *Biosens. Bioelectron.* **2002**, *17*, 345−359.

(7) Kim, W. H.; Mäkinen, A. J.; Nikolov, N.; Shashidhar, R.; Kim, H.; Kafafi, Z. H. Molecular Organic Light-Emitting Diodes Using Highly

DOI: 10.1021/acs.jpcc.6b09642
J. Phys. Chem. C 2016, 120, 25977−25984

Conducting Polymers as Anodes. *Appl. Phys. Lett.* **2002**, *80*, 3844−3846.
(8) Yu, G.; Gao, J.; Hummelen, J. C.; Wudl, F.; Heeger, A. J. Polymer Photovoltaic Cells: Enhanced Efficiencies via a Network of Internal Donor-Acceptor Heterojunctions. *Science* **1995**, *270*, 1789−1791.
(9) Tsumura, A.; Koezuka, H.; Ando, T. Macromolecular Electronic Device: Field-Effect Transistor with a Polythiophene Thin Film. *Appl. Phys. Lett.* **1986**, *49*, 1210−1212.
(10) Nalwa, H. S. *Handbook of Organic Conductive Molecules and Polymers: Vol. 4 Conductive Polymers: Transport, Photophysics and Applications*; John Wiley & Sons Ltd.: Chichester, UK, 1997.
(11) Liu, C. Y.; Chou, J. C.; Liao, Y. H.; Yang, C. J.; Huang, C. J.; Cheng, T. Y.; Hu, J. E.; Chou, H. T. Proceedings of the World Congress on Engineering 2013, Vol II, WCE 2013, London, U.K., July 3−5, 2013.
(12) March, J. *Advanced Organic Chemistry: Reactions, Mechanisms, and Structure*, 4th ed.; John Wiley & Sons, Inc.: New York, 1992.
(13) Takano, T.; Masunaga, H.; Fujiwara, A.; Okuzaki, H.; Sasaki, T. PEDOT Nanocrystal in Highly Conductive PEDOT:PSS Polymer Films. *Macromolecules* **2012**, *45*, 3859−3865.
(14) Latessa, G.; Brunetti, F.; Reale, A.; Saggio, G.; Di Carlo, A. Piezoresistive Behaviour of Flexible PEDOT:PSS Based Sensors. *Sens. Actuators, B* **2009**, *139*, 304−309.
(15) Kirchmeyer, S.; Reuter, K. Scientific Importance, Properties and Growing Applications of Poly(3,4-ethylenedioxythiophene). *J. Mater. Chem.* **2005**, *15*, 2077−2088.
(16) Aernouts, T.; Vanlaeke, P.; Geens, W.; Poortmans, J.; Heremans, P.; Borghs, S.; Mertens, R.; Andriessen, R.; Leenders, L. Printable Anodes for Flexible Organic Solar Cell Modules. *Thin Solid Films* **2004**, *451−452*, 22−25.
(17) Hu, B.; Li, D.; Manandharm, P.; Fan, Q.; Kasilingam, D.; Calvert, P. CNT/Conducting Polymer Composite Conductors Impart High Flexibility to Textile Electroluminescent Devices. *J. Mater. Chem.* **2012**, *22*, 1598−1605.
(18) Kudoh, Y.; Akami, K.; Matsuya, Y. Solid Electrolytic Capacitor with Highly Stable Conducting Polymer as a Counter Electrode. *Synth. Met.* **1999**, *102*, 973−974.
(19) Kim, Y. H.; Lee, J.; Hofmann, S.; Gather, M. C.; Müller-Meskamp, L.; Leo, K. Achieving High Efficiency and Improved Stability in ITO-Free Transparent Organic Light-Emitting Diodes with Conductive Polymer Electrodes. *Adv. Funct. Mater.* **2013**, *23*, 3763−3769.
(20) Huang, D. M.; Mauger, S. A.; Friedrich, S.; George, S. J.; Dumitriu-LaGrange, D.; Yoon, S.; Moulé, A. J. The Consequences of Interface Mixing on Organic Photovoltaic Device Characteristics. *Adv. Funct. Mater.* **2011**, *21*, 1657−1665.
(21) Sun, J.; Zhang, B.; Katz, H. E. Materials for Printable, Transparent, and Low-Voltage Transistors. *Adv. Funct. Mater.* **2011**, *21*, 29−45.
(22) Greco, F.; Zucca, A.; Taccola, S.; Menciassi, A.; Fujie, T.; Haniuda, H.; Takeoka, S.; Dario, P.; Mattoli, V. Ultra-Thin Conductive Free-Standing PEDOT/PSS Nanofilms. *Soft Matter* **2011**, *7*, 10642−10650.
(23) Del Valle, L. J.; Aradilla, D.; Oliver, R.; Sepulcre, F.; Gamez, A.; Armelin, E.; Alemàn, C.; Estrany, F. Cellular Adhesion and Proliferation on Poly(3,4-ethylenedioxythiophene): Benefits in the Electroactivity of the Conducting Polymer. *Eur. Polym. J.* **2007**, *43*, 2342−2349.
(24) Ouyang, J.; Chu, C. W.; Chen, F. C.; Xu, Q.; Yang, Y. High-Conductivity Poly(3,4-ethylenedioxythiophene):Poly(styrene sulfonate) Film and Its Application in Polymer Optoelectronic Devices. *Adv. Funct. Mater.* **2005**, *15*, 203−208.
(25) Mengistie, D. A.; Wang, P. C.; Chu, C. W. Effect of Molecular Weight of Additives on the Conductivity of PEDOT:PSS and Efficiency for ITO-Free Organic Solar Cells. *J. Mater. Chem. A* **2013**, *1*, 9907−9915.
(26) Chou, T. R.; Chen, S. H.; Chiang, Y. T.; Lin, Y. T.; Chao, C. Y. Highly Conductive PEDOT:PSS Films by Post-Treatment with Dimethyl Sulfoxide for ITO-Free Liquid Crystal Display. *J. Mater. Chem. C* **2015**, *3*, 3760−3766.
(27) Kim, H.; Lee, J.; Ok, S.; Choe, Y. Effects of Pentacene-Doped PEDOT:PSS as a Hole-Conducting Layer on the Performance Characteristics of Polymer Photovoltaic Cells. *Nanoscale Res. Lett.* **2012**, *7*, 5.
(28) Xia, Y.; Ouyang, J. PEDOT:PSS Films with Significantly Enhanced Conductivities Induced by Preferential Solvation with Cosolvents and Their Application in Polymer Photovoltaic Cells. *J. Mater. Chem.* **2011**, *21*, 4927−4936.
(29) Lang, U.; Rust, P.; Schoberle, B.; Dual, J. Piezoresistive Properties of PEDOT:PSS. *Microelectron. Eng.* **2009**, *86*, 330−334.
(30) Li, Y.; Deng, C.; Yang, M. A Novel Surface Acoustic Wave-Impedance Humidity Sensor Based on the Composite of Polyaniline and Poly(vinyl alcohol) with a Capability of Detecting Low Humidity. *Sens. Actuators, B* **2012**, *165*, 7−12.
(31) Zou, Z.; Kai, J.; Rust, M. J.; Han, J.; Ahn, C. H. Functionalized Nano Interdigitated Electrodes Arrays on Polymer with Integrated Microfluidics for Direct Bio-Affinity Sensing Using Impedimetric Measurement. *Sens. Actuators, A* **2007**, *136*, 518−526.
(32) Mamishev, A. V.; Sundara-Rajan, K.; Yang, F.; Du, Y.; Zahn, M. Interdigital Sensors and Transducers. *Proc. IEEE* **2004**, *92*, 808−845.
(33) Fasth, C.; Fuhrer, A.; Björk, M. T.; Samuelson, L. Tunable Double Quantum Dots in InAs Nanowires Defined by Local Gate Electrodes. *Nano Lett.* **2005**, *5*, 1487−1490.
(34) Wang, J. C.; Karmakar, R. S.; Lu, Y. J.; Huang, C. Y.; Wei, K. C. Characterization of Piezoresistive PEDOT:PSS Pressure Sensors with Inter-Digitated and Cross-Point Electrode Structures. *Sensors* **2015**, *15*, 818−831.
(35) Hillebrandt, H.; Wiegand, G.; Tanaka, M.; Sackmann, E. High Electric Resistance Polymer/Lipid Composite Films on Indium−Tin−Oxide Electrodes. *Langmuir* **1999**, *15*, 8451−8459.
(36) Hillebrandt, H.; Tanaka, M. Electrochemical Characterization of Self-Assembled Alkylsiloxane Monolayers on Indium−Tin Oxide (ITO) Semiconductor Electrodes. *J. Phys. Chem. B* **2001**, *105*, 4270−4276.
(37) Kim, H.; Lee, J.; Park, C. Surface Characterization of O_2-Plasma-Treated Indium-Tin-Oxide (ITO) Anodes for Organic Light-Emitting-Device Applications. *J. Korean Phys. Soc.* **2002**, *41*, 395−399.
(38) MatWeb Material Property Data. http://www.matweb.com/search/datasheet.aspx?matguid=e423305073784d4481bdcefea6c97961&ckck=1 (accessed Oct. 18, 2016).
(39) Stöcker, T.; Köhler, A.; Moos, R. Why Does the Electrical Conductivity in PEDOT:PSS Decrease with PSS Content? A Study Combining Thermoelectric Measurements with Impedance Spectroscopy. *J. Polym. Sci., Part B: Polym. Phys.* **2012**, *50*, 976−983.
(40) Fogler, M. M.; Teber, S.; Shklovskii, B. I. Variable-Range Hopping in Quasi-One-Dimensional Electron Crystals. *Phys. Rev. B: Condens. Matter Mater. Phys.* **2004**, *69*, 035413.
(41) Nardes, A. M.; Kemerink, M.; Janssen, R. A. J.; Bastiaansen, J. A. M.; Kiggen, N. M. M.; Langeveld, B. M. W.; van Breemen, A. J. J. M.; de Kok, M. M. Microscopic Understanding of the Anisotropic Conductivity of PEDOT:PSS Thin Films. *Adv. Mater.* **2007**, *19*, 1196−1200.
(42) Bai, Y.; Wu, H.; Wu, R.; Zhang, Y.; Deng, N.; Yu, Z.; Qian, H. Study of Multi-level Characteristics for 3D Vertical Resistive Switching Memory. *Sci. Rep.* **2014**, *4*, 5780.
(43) Nardes, A. M.; Kemerink, M.; Janssen, R. A. J. Anisotropic Hopping Conduction in Spin-Coated PEDOT:PSS Thin Films. *Phys. Rev. B: Condens. Matter Mater. Phys.* **2007**, *76*, 085208.
(44) Bachmann, J.; Horton, R.; van der Ploeg, R. R.; Woche, S. Modified Sessile Drop Method for Assessing Initial Soil−Water Contact Angle of Sandy Soil. *Soil Sci. Soc. Am. J.* **2000**, *64*, 564−567.
(45) Yin, H. E.; Huang, F. H.; Chiu, W. Y. Hydrophobic and Flexible Conductive Films Consisting of PEDOT:PSS-PBA/Fluorine-Modified Silica and Their Performance in Weather Stability. *J. Mater. Chem.* **2012**, *22*, 14042−14051.

DOI: 10.1021/acs.jpcc.6b09642
J. Phys. Chem. C 2016, 120, 25977−25984

(46) Moulder, J. F.; Stickle, W. F.; 'Sobol, P. E.; Bomben, K. D. *Handbook of X-ray Photoelectron Spectroscopy*; Perkin-Elmer Corp., Physical Electronics Division: Eden Prairie, MN, 1992.
(47) Ilieva, M.; Tsakova, V.; Vuchkov, N.; Temelkov, K.; Sabotinov, N. Microscopy—advanced Tools for Tomorrow's Materials, Autumn School on Materials Science and Electron Microscopy, Berlin, October 8−11, 2007.
(48) Spanninga, S. A.; Martin, D. C.; Chen, Z. X-ray Photoelectron Spectroscopy Study of Counterion Incorporation in Poly(3,4-ethylenedioxythiophene) (PEDOT) 2: Polyanion Effect, Toluenesulfonate, and Small Anions. *J. Phys. Chem. C* **2010**, *114*, 14992.
(49) Crispin, X.; Marciniak, S.; Osikowicz, W.; Zotti, G.; van der Gon, A. W. D.; Louwet, F.; Fahlman, M.; Groenendaal, L.; De Schryver, F.; Salaneck, W. R. Conductivity, Morphology, Interfacial Chemistry, and Stability of Poly(3,4-ethylene dioxythiophene)−Poly(styrene sulfonate): A Photoelectron Spectroscopy Study. *J. Polym. Sci., Part B: Polym. Phys.* **2003**, *41*, 2561−2583.
(50) Greczynski, G.; Kugler, T.; Salaneck, W. R. Characterization of the PEDOT-PSS System by Means of X-ray and Ultraviolet Photoelectron Spectroscopy. *Thin Solid Films* **1999**, *354*, 129−135.
(51) Beamson, G.; Briggs, D. *High Resolution XPS of Organic Polymers*; John Wiley and Sons: Chichester, UK, 1992.
(52) d'Agostino, R.; Favia, P.; Oehr, C.; Wertheimer, M. R. *Plasma Processes and Polymers: 16th International Symposium on Plasma Chemistry*; John Wiley and Sons: Chichester, UK, 2005.
(53) Briggs, D.; Beamson, G. XPS Studies of the Oxygen 1s and 2s Levels in a Wide Range of Functional Polymers. *Anal. Chem.* **1993**, *65*, 1517−1523.
(54) Petraki, F.; Kennou, S.; Nespurek, S.; Biler, M. A Spectroscopic Study for the Application of a PEDOT-Type Material as Buffer Layer in Electronic Devices. *Org. Electron.* **2010**, *11*, 1423−1431.
(55) Wang, J. C.; Lin, Y. H.; Ye, Y. R.; Lai, C. S.; Ai, C. F.; Tsai, W. F. Hybrid Anion and Cation Ion Sensors with Samarium Oxide Sensing Membrane Treated by Nitrogen Plasma Immersion Ion Implantation. *Sens. Actuators, B* **2014**, *191*, 666−672.
(56) Chang, S. H.; Chiang, C. H.; Kao, F. S.; Tien, C. L.; Wu, C. G. Unraveling the Enhanced Electrical Conductivity of PEDOT:PSS Thin Films for ITO-Free Organic Photovoltaics. *IEEE Photon. J.* **2014**, *6*, 8400307.
(57) Lambert, J. B.; Gronert, S.; Shurvell, H. F.; Lightner, D. A. *Organic Structural Spectroscopy*, 2nd ed.; Prentice Hall: Upper Saddle River, NJ, 2011.
(58) Greczynski, G.; Kugler, T.; Keil, M.; Osikowicz, W.; Fahlman, M.; Salaneck, R. W. Photoelectron Spectroscopy of Thin Films of PEDOT−PSS Conjugated Polymer Blend: A Mini-Review and Some New Results. *J. Electron Spectrosc. Relat. Phenom.* **2001**, *121*, 1−17.
(59) Cao, Z. X.; Oechsner, H. Effect of Concurrent N_2^+ and N^+ Ion Bombardment on the Plasma-Assisted Deposition of Carbon Nitride Thin Film. *J. Vac. Sci. Technol., A* **2004**, *22*, 321−323.
(60) Vitoratos, E.; Sakkopoulos, S.; Dalas, E.; Paliatsas, N.; Karageorgopoulos, D.; Petraki, F.; Kennou, S.; Choulis, S. A. Thermal Degradation Mechanisms of PEDOT:PSS. *Org. Electron.* **2009**, *10*, 61−66.
(61) Saito, S.; Yukawa, M. Interactions of Polymers and Cationic Surfactants with Thiocyanate as Counterions. *J. Colloid Interface Sci.* **1969**, *30*, 211−218.
(62) Kim, J. Y.; Jung, J. H.; Lee, D. E.; Joo, J. Enhancement of Electrical Conductivity of Poly(3,4-ethylenedioxythiophene)/Poly(4-styrenesulfonate) by a Change of Solvents. *Synth. Met.* **2002**, *126*, 311−316.

■ NOTE ADDED AFTER ASAP PUBLICATION

This paper was published to the Web on November 9, 2016, with an error in Figure 6. This was corrected in the version published to the Web on November 17, 2016.

DOI: 10.1021/acs.jpcc.6b09642
J. Phys. Chem. C 2016, 120, 25977−25984